IEEE Access
Multidisciplinary | Rapid Review | Open Access Journal

Received March 12, 2019, accepted April 2, 2019, date of publication April 15, 2019, date of current version April 29, 2019.

*Digital Object Identifier 10.1109/ACCESS.2019.2911301*

# A Distributed Coevolution Algorithm for Black Box Optimization of Demand Response

**XINYUAN ZHANG[1], (Student Member, IEEE), YUE-JIAO GONG[2], (Member, IEEE), YUREN ZHOU[1], (Member, IEEE), AND YING LIN[3], (Member, IEEE)**

[1]School of Data and Computer Science, Sun Yat-sen University, Guangzhou 510006, China
[2]School of Computer Science and Engineering, South China University of Technology, Guangzhou 510006, China
[3]Department of Psychology, Sun Yat-sen University, Guangzhou 510006, China

Corresponding author: Yue-jiao Gong (gongyuejiao@gmail.com)

This work was supported by the National Natural Science Foundation of China under Grant 61873095, Grant 61772569, Grant 61773410, and Grant U1701267.

**ABSTRACT** Demand side management is an efficient way of reducing the grid fluctuation and enhancing the net profit in the smart grid. As the increasing complexity of the real-world applications, e.g., NP-hard and non-polynomial problems, a distributed coevolution algorithm is proposed to cope with this challenge. In the proposed algorithm, the management system is modeled as a hierarchical structure. The user side locates at the lowest level and upper levels represent the system operators. The system operators manage users' energy consumption behavior through the real-time pricing strategy. The genetic algorithm and particle swarm optimization are modified to play the role of the smart scheduler and the smart pricing generator. The end users conduct appliance commitment using the smart scheduler which considers the users' comfort level and the electricity cost. The decision of the lower level depends directly on the real-time pricing strategy released by its adjacent upper level. The real-time pricing is developed by the smart pricing generator which considers the net profit and the grid fluctuation. Three types of experiments are conducted on a distributed platform to investigate and ascertain the performance of the proposed algorithm. For the operator side, the experimental results indicate that the proposed algorithm improves the grid fluctuation, and enhances the net profit. As for the user side, it improves the comfort level and achieves budget saving.

**INDEX TERMS** Demand side management, distributed co-evolutionary algorithm, hierarchical structure, real-time pricing.

## I. INTRODUCTION

The objective of the smart grid is constructing an efficient, flexible, economic, and reliable energy system which satisfies numerous requirements of users and system operators. In order to achieve the objectives, the demand response (DR) is proposed to intelligently regulate users' energy consumption behavior, which improves the generation cost, the grid fluctuation, the transmission congestion and the supply-demand mismatch [1]. Among kinds of different demand-response programs [2], [3], we focus on the real-time pricing (RTP) scheme [4], [5]. In contrast to the legacy flat electricity price, the RTP scheme provides users with different electricity prices at different time slots, which naturally drives users to manage their energy consumption schedule dynamically in response to the time varying electricity price [6], [7].

The associate editor coordinating the review of this manuscript and approving it for publication was Dongbo Zhao.

As an important part of the smart grid, microgrid has been wildly studied in [8]–[10]. The microgrid features a small power system including an aggregation of the end users and the distributed energy resources which is under the coordination of a microgrid operator (MGO). The microgrid is capable of operating independently under emergency circumstance, or being in conjunction with the distribution or transmission network under normal circumstance. When operating in cooperative mode, the MGO can be viewed as a single entity responding to demand response signals granted by upper management units such as Independent System Operator (ISO) or Regional Transmission Organization (RTO) [11], [12]. Therefore, the management system naturally forms a hierarchical structure where the MGO participates in the DR process coordinated by its adjacent upper ISO and the end users participate in the one coordinated by its upper MGO.

In this paper, we adopt a hierarchical management structure. DR is applied between different levels, e.g., ISO and MGO, or MGO and end users. In the hierarchical management structure, each parent entity determines a piece of RTP and their child entities upload their energy consumption schemes after conducting the appliance commitment with respect to the RTP information. This hierarchical structure obtains promising improvement in terms of robustness and economic benefit. Grid fluctuation from the lower level can be smoothened level by level through specific RTP strategy, and each subtree can operate in the island mode in case of the emergency situation. Besides, reasonable RTP strategy makes contributions to improving the economic benefit of ISO or MGO. As for user side, the proposed generic appliance commitment algorithm achieves cost reduction and while ensuring an acceptable degree of comfort.

In order to balance the interests between the stakeholders of different levels, we adopt the 1-leader, N-followers Stackelberg game model [13]–[15] as the basic gaming rule for the gaming process. The Stackelberg rule is adopted to cope with the multilevel optimization problem [16], [17] where hierarchical management structure is considered. For system operators, the objectives of the upper-levels are increasing the profit and the reliability [18], [19]. As for the end users, the objective is enhancing their utility function [20], [21] while ensuring an acceptable degree of the comfort level. There exist numerous constraints within different levels: 1) for the ISO or MGO level, we consider the security of electrical network, and 2) for user level, numerous types of appliances, e.g., discharging or charging of local storage, such as the plug-in hybrid electrical vehicles (PHEVs), are included with their respective operating constraints.

The objective and constraint functions of different levels can be modeled as different complex problems, such as convex, non-convex. The existing optimization algorithms of DR achieve promising performance in solving the convex optimization problems [22]. However, the complexity of the DR optimization problems increases [23] as the integration of various components. The non-convex [24], [29], NP-hard [31], and DR problems with uncertainty [32], e.g., ''black swan event'' [33] have drawn attentions recently. The existing optimization algorithm is unsuitable for solving the complex optimization problems. It is therefore desirable to design a more generic framework that is capable of handling this complex landscape of problem space. Without the loss of generality, the DR optimization problem is considered as a black box problem in this paper. Owing to the success in solving complex problems, evolutionary algorithms (EAs) have been applied to cope with the challenges in smart grid [25], [26]. We adopt EAs as the main optimizers of the proposed framework. Furthermore, in order to deal with the gaming rules between operators and users, classical game theory models are considered when designing a specific optimization algorithm [27], [28]. Along with this line of thinking, we view the gaming process between different levels as a co-evolutionary gaming process, which is also motivated by the evolutionary game theory (EGT) [36]. Compared with new evolutionary techniques (e.g., extremal optimization [37], [38]), the performance of genetic algorithm (GA) and particle swarm optimization (PSO) has been validated through a broad class of optimization problems. In this paper, we adopt and modify GA and PSO as the optimizers.

In order to achieve the above-mentioned multi-win situation of ISO, MGOs, and end users, a distributed co-evolutionary algorithm (DCoEA) is developed with the following features and benefits:

- A more generic algorithm: the distributed optimization algorithm is designed based on the evolutionary algorithms, which is capable of handling the black box optimization of demand response;
- The protection of end users' privacy: In the distributed optimization algorithm, system operators requires residential load profile other than the parameters of their appliances;
- Environmental protection: the proposed management system allows users selling their electricity back to the grid, and therefore it encourages end users to use the renewable energy resources;
- The win-win situation: for system operator, the distributed optimization algorithm improves the grid reliability and the economic benefit, whilst it reduces the electricity cost and ensures a high comfort level of end users.

The rest of this paper is organized as follows: we develop the distributed co-evolutionary algorithm in section II. In section III, three types of experiments are conducted in order to ascertain the effectiveness of the proposed algorithm. Finally, conclusions are drawn in section IV.

## II. MODEL OF THE DISTRIBUTED CO-EVOLUTIONARY ALGORITHM

In this section, we first give the management structure of the considered smart grid system. After that, the formulation of the DR optimization problem is given. We view this optimization problem as a black box optimization problem in order to ensure the generality. In the management structure, each node is able to make decision, i.e., conduct optimization. The communication process between different levels of the management structure is modeled as a gaming process. Considering the limited computational resources of the end users, the end users are supposed to be bounded rationality. In the proposed distributed algorithm, the gaming process is simulated by a coevolutionary process. For level I and level II, level II and user level, different optimizers are designed to satisfy the corresponding requirements of different levels.

In this paper, the optimizers play the roles of smart pricing generator and the smart scheduler for system operator and end users, respectively. The co-evolutionary process of optimizers is expected to simulate the infinite repeated game. In each game round, the smart pricing generator releases a pricing vector to the smart scheduler, and the smart scheduler

generate load profile for each end user. Assuming that the optimization problems of system operator and end users are modeled as multi-objective optimization problems, the gaming process will be quite complicated. Without the loss of fairness, we consider a grid with one system operator and $N$ end users. In each game round, each smart scheduler obtains $M$ load profiles for each pricing vector. The global load profile requires the combination of $N$ end users' local profiles. However, there exist $M^N$ combinations. The evaluation of $M^N$ global load profiles requires too many computational resources. Therefore, the black box optimization problem is modeled as a single objective problem in this paper. The detail of the proposed distributed co-evolutionary algorithm is given in the following subsections.

### A. HIERARCHICAL STRUCTURE OF THE MANAGEMENT SYSTEM

We adopt a hierarchical structure of the management system of smart grid in this paper, which is shown in Fig. 1(a). Level I and level II represent system operators, whilst level III represents the end users. The hierarchical structure is widely used in smart grid [30], [34]. The hierarchical structure is adopted because it naturally follows the practical administrative classification of numerous countries. Furthermore, the hierarchical structure enhances the grid reliability through the smoothing of the grid fluctuation level by level. The decentralized structure allows users conducting appliance commitment in a distributed manner, which is a way of protecting the users' privacy [33], [35].

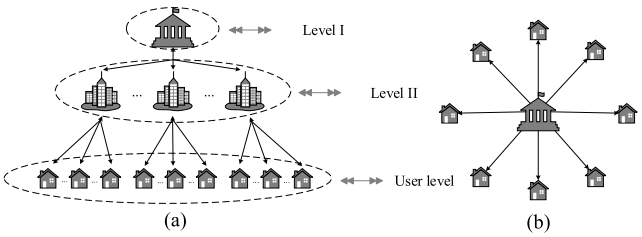


**FIGURE 1.** Sketch of the hierarchical structure (a) and centralized structure (b). The patent and leaf nodes represent system operators and end users, respectively. Each node owns the ability to perform optimization of the demand response.

Instead of fully formulating all issues influencing the behavior of smart grid, we simplify our proposed model by making the following assumptions without the loss of generality: 1) The highest level is considered as a combination of the power plant, the wholesaler, and the ISO (PWISO), which provides electricity for the lowest level, and is responsible for the security of the whole grid, 2) the internal level is considered as a combination of retailer and MGO (RMGO), which provides electricity for lower level by purchasing electricity from its upper level and is responsible for the security of the sub-grids, 3) the end users have the ability of generating energy, therefore, they can sell electricity back to the grid, and 4) the ISO, the RMGO and the end users have computational resources to conduct its own optimization.

The proposed hierarchical structure is derived from the administrative classification, the higher the level is, the higher authority it owns. Level I to level II focus on different objectives of the smart grid. Level II can be viewed as auxiliary system operators cooperated with level I in order to reduce the grid fluctuation. In Fig. 1(a), higher level regulates the energy consumption of its adjacent lower level through the real-time pricing strategy. Therefore, the grid fluctuation of each level can be smoothened level by level by a specific designed real-time pricing strategy. In Fig. 1, this hierarchical structure is able to reduce the scheduling burden of level II. The computational burden of the decentralized system can be significantly reduced compared with the centralized structure shown as Fig. 1(b). Fig. 1(b) depicts the centralized structure, the end users communicate directly with the data center. The data center is responsible for the optimization of the whole grid, which is a heavy burden in terms of computational resource.

### B. THE DISTRIBUTED CO-EVOLUTIONARY ALGORITHM

Based on the above-mentioned hierarchical structure, we proposed a distributed coevolutionary algorithm denoted by DCoEA. The framework of DCoEA is given in Fig. 2 where the standard particle swarm optimization (SPSO) [42] and the genetic algorithm (GA) [43] are adopted and modified as the smart pricing generator and the smart scheduler for the system operators and the end users, respectively. Fig. 2(a) represents the global coevolutionary process. The solid and dashed arrows represent propagation directions of the load profile and pricing information, respectively. For each round of the gaming process, there are two stages: 1) the pricing information is released from level I to end users level by level, and 2) the feedback of load profile is uploaded from end user to level I level by level. In the first stage, the PWISO of level I releases pricing information to the RMGOs of level II and wait for the feedback of load profile. Then, the RMGOs of level II release pricing information to its end users. It should be noted that the pricing information keeps identical within the same level to ensure the fairness. In second stage, each user determines their load scheduling strategy, i.e., load profile, according to the pricing information and uploads the load profile back to the corresponding RMGOs of level II. Then, the RMGOs of level II gather the feedback of load profile and evaluate their released pricing strategy with a given objective function. Similarly, PWISO of I gathers the feedbacks and evaluates their objective functions successively.

The structure of Fig. 2(a) is a perfect multi-furcating tree. Considering leaf $i$, the smart scheduler develops user's energy consumption scheme, represented by a vector $\boldsymbol{l_i} = (l_{i,1}, l_{i,2}, \ldots, l_{i,H})$, according to the real-time pricing $\boldsymbol{P_i} = (p_{i,1}, p_{i,2}, \ldots, p_{i,H})$.

The scheduling horizon is uniformly divided into $H$ time slots. For time slot $[t_k, t_{k+1}]$ $(k = \{0, 1, \ldots, H-1\})$, we consider the length of time slot $t_{k+1} - t_k$ as unit time. The pricing vector $\boldsymbol{P_i}$ is developed by the smart pricing generator. For the $j$th dimension of $\boldsymbol{P_i}$, $p_{i,j}$ is a 2-tuples $(p_{i,j,s}, p_{i,j,p})$

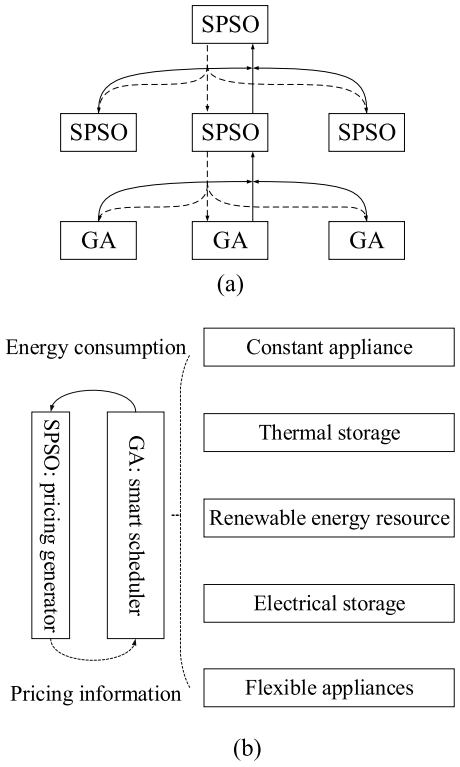


**FIGURE 2.** Framework of the communication structure of the distributed coevolutionary algorithm between adjacent levels. (a) The global coevolution structure between system operators and end users. The solid and dashed arrows represent propagation directions of the load profile and pricing information, respectively. (b) The coevolutionary process between system operator and end users. The system operators release pricing information through the SPSO-based pricing generator. The end users conduct commitment using the GA-based smart scheduler.

where $p_{i,j,s}$ and $p_{i,j,p}$ represent the selling and purchasing electricity price, respectively. The objective function of leaf $i$ is given by equation (1) where $\rho(l_{,j})$ is a penalty function if the total power consumption exceeds the upper limit of household grid. Function $f_{i,comf}$ and $f_{i,cost}$ represent the degree of comfort level and the electricity cost of the $i$th end user. Temperature $T_{i,\alpha}$ is the desired indoor temperature. Temperature $T_{i,t}$ is the predictive temperature of a house at the $t$th time slot, which can be computed with a given air-conditioning load vector. $\chi_1$ is adopted to cope with the problem of the order of magnitude between $f_{i,comf}$ and $f_{i,cost}$.

$$f_{i,comf,\cos t} = \chi_1 \cdot f_{i,comf} + f_{i,cost} \tag{1}$$

$$f_{i,\cos t} = \sum_{j=1}^{H} sel(p_{i,j}, l_{i,j}) \cdot l_{i,j} \cdot \rho(l_{i,j}) \tag{2}$$

$$\rho(l_{i,j}) = \begin{cases} 1.0 & if\ l_{i,j} < l_m \\ 10 & otherwise \end{cases} \tag{3}$$

$$sel(p_{i,j}, l_{i,j}) = \begin{cases} p_{i,j,s} & if\ l_{i,j} \geq 0 \\ p_{i,j,p} & otherwise \end{cases} \tag{4}$$

$$f_{i,comf} = \sum_{t=1}^{H} (T_{i,t} - T_{i,\alpha})^2 \tag{5}$$

For internal node $k$ and its parent node, we use a 2-tuples $(\boldsymbol{p}_k, \boldsymbol{q}_k)$ to represent its received and released price vectors. For the $j$th dimension of $\boldsymbol{q}_k$, $q_{k,j}$ is also a 2-tuples $(q_{k,j,s}, q_{k,j,p})$ with the same definition of $p_{i,j}$. Objective function of internal nodes is different from that of leaf nodes, which considers two respects: 1) the grid fluctuation $f_{k,flu,}$, and 2) the profit $f_{k,prof}$. The objective function of internal node $k$ can be formulated as equation (6) where $f_{k,cost}$ is the cost of node $k$.

$$f_{k,flu,prof} = \chi_2 \cdot f_{k,\,flu} + f_{k,prof} \tag{6}$$

$$f_{k,\,flu} = \max_{t\in\{1,2,\ldots,H\}} \{L_{k,t}\} \cdot H \cdot (\sum_{t=1}^{H} L_{k,t})^{-1} \tag{7}$$

$$L_{k,t} = \sum_{m\in C^k} l_{m,t} \tag{8}$$

$$f_{k,prof} = \sum_{m\in C^k} f_{m,cost} - f_{k,cost} \tag{9}$$

$$f_{m,cost} = \begin{cases} \sum_{t=0}^{H} \mu(L_{m,t}) & for\ root\ nodes \\ \sum_{t=1}^{H} sel(p_{m,t}, l_{m,t}) \cdot l_{m,t} & otherwise \end{cases} \tag{10}$$

Load $L_{m,t}$ is the load summation of its child nodes denoted by $C^k$. Similarly, $\chi_2$ is adopted to cope with the problem of the order of the magnitude between $f_{k,flu}$ and $f_{k,prof}$. For the root node, i.e., PWISO of level I, the classical quadratic function [39] given by equation (11) is adopted as cost function of generation cost.

$$\mu(L_{m,t}) = a{L_{m,t}}^2 + bL_{m,t} + c \tag{11}$$

### C. CO-EVOLUTION BETWEEN ADJACENT LEVELS

In this section, we introduce the coevolutionary process between adjacent levels in detail. Take the three-level structure of Fig. 2 as an example, the co-evolutionary process can be divided into two categories: 1) coevolutionary process between the modified SPSO and SPSO, i.e., level I and level II, and 2) coevolutionary process between SPSO and GA, i.e., level II and user level.

Considering node $k$ of level I and its child nodes of level II, Fig. 3 shows the specific framework of the co-evolutionary process between SPSO (level I) and SPSO (level II). Firstly, the particle swarms of level I and level II are randomly initialized. Each particle is encoded as a pricing vector with the same definition of $\boldsymbol{q}_k$. Then, the trial pricing vectors of level I are released to its child nodes of level II, and RMGOs of level II keep the pricing vectors for the computation of purchasing cost. After that, the smart pricing generator of RMGO develops their own trial price vectors and broadcast them to end users.

Considering node $k$ of level II and all its child nodes $C^k$, Fig. 4 shows the co-evolutionary process between SPSO (level II) and GA (user level). For each evolutionary iteration, SPSO broadcasts its trial price vectors to GAs, and each GA

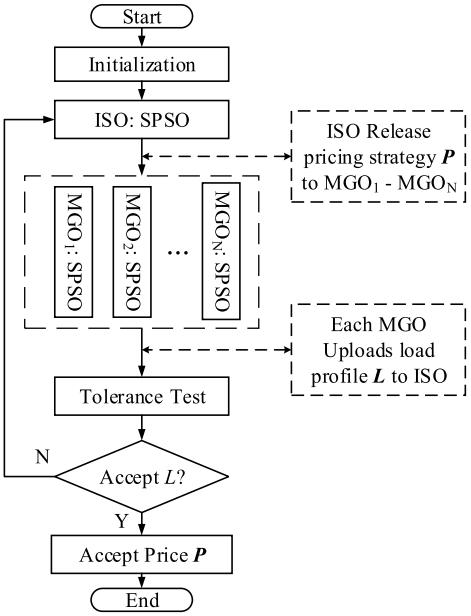


**FIGURE 3.** Detail of the co-evolutionary process between level I and level II. The ISO releases pricing strategy to its adjacent lower level, i.e., MGO. The MGOs conduct their own optimization in a parallel manner, and then wait the feedback of the load profile of the end users.

searches a near optimal load scheduling strategy with objective function as equation (1). After gathering the feedback $\boldsymbol{L} = (L_{k,1}, L_{k,2}, \ldots, L_{k,H})$, the fitness of the trial pricing vector can be evaluated according to equation (6). If load $\boldsymbol{L}$ accesses the tolerance test, it will be uploaded to PWISO and the trial price vectors of level I can also be evaluated by equation (6). Then, each particle updates its velocity, position, and historical information according to the new fitness.

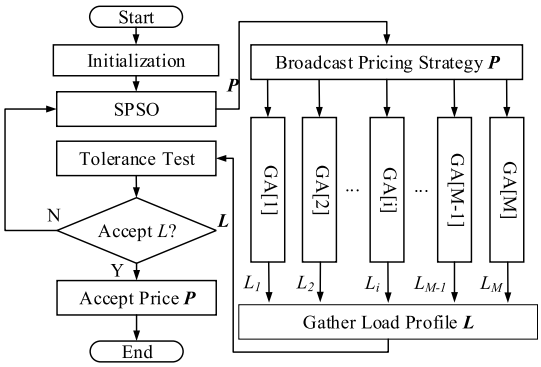


**FIGURE 4.** Detail of the co-evolutionary process between level II and user level. The MGO releases pricing strategy and the users conduct appliance commitment based on the current pricing vector. The modified GA is parallelly executed to solve the optimization of the user side.

As can be noted from Fig. 3 and Fig. 4, the evaluation process of objective functions between adjacent levels works in a cooperative mode. This co-evolutionary process is time consuming in finding the optimal solution. Therefore, a simple auxiliary operation called tolerance test is expected to control the computational time. SPSO can be terminated in advance

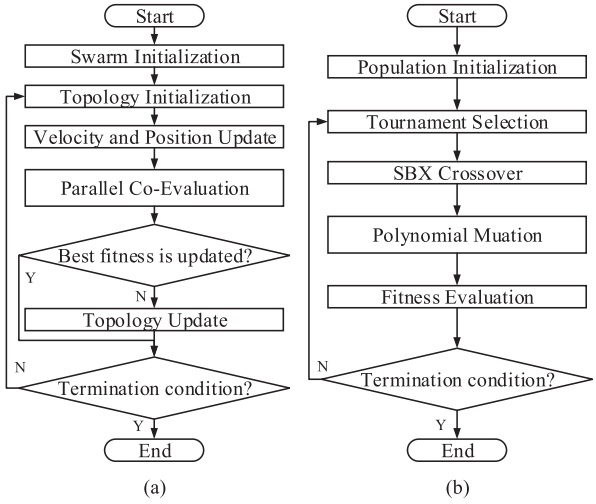


**FIGURE 5.** The framework of SPSO and GA. (a) The SPSO. (b) The GA. The maximum fitness evaluations are adopted as the termination condition.

before reaching a given maximum function evaluations (FEs) if the feedback satisfies the requirements as follows:

$$f_{k,flu} \leq \varepsilon_m \tag{12}$$

$$f_{k,prof} \geq f_m \tag{13}$$

where $\varepsilon_m$ and $f_m$ represent the acceptable maximum grid fluctuation and minimum acceptable profit. These two threshold values are user-defined according to different application scenes. Fig. 5 (a) and (b) show the framework of the modified SPSO and GA, where co-evolutionary process takes place in the operation of the parallel co-evaluation.

As can be noted from Fig. 3 and Fig. 4, the optimizers of different levels work in a cooperative co-evolutionary manner. Without the loss of generality, we assume the numbers of the maximum fitness evaluations (FEs) are $K_1$, $K_2$, and $K_3$ for the optimizers of level I, level II, and user level, respectively. The computational complexity is $O(K_1 \cdot NK_2 \cdot NMK_3)$ if the proposed algorithm is implemented in the way of serial mode. In this paper, we implement the proposed algorithm in a parallel manner. The optimizers of the same level conduct optimization task simultaneously, i.e., the SPSOs and GAs are conducted in parallel. The time complexity is accordingly reduced to $O(K_1 \cdot K_2 \cdot K_3)$.

### D. APPLIANCE COMMITMENT FOR HOUSEHOLD LOAD SCHEDULING USING GA

We introduce the appliance commitment of user level in this subsection. A modified GA using hybrid encodings is designed to obtain an acceptable energy consumption scheme with the objective defined by equation (1). For the end users, we have the following assumptions: 1) all users own two kinds of storages, electrical and thermal storage, and 2) quite a few users are able to generate electricity using photovoltaic (PV) generator and allowed to sell electricity back

to the grid. In this paper, four typical types of appliance are considered as follows:

a) The flexible appliances, such as air-conditioning, and washing machine, which achieve high controllability and directly influence the comfort of users.
b) The electrical storage, such as PHEV battery. From the point of view of user side, the scheduling of battery is expected to reduce the electricity expense, whilst it contributes to the reduction of the grid fluctuation implicitly.
c) The constant appliance, such as refrigerator, lighting system, and cooker, which represent the constant behavior of users.
d) The renewable energy resources, such as the PV generator. As can be noted from the proposed framework, the real-time pricing scheme released by system operator consists of selling and purchasing price. Therefore, it encourages users to sell their surplus electricity back to grid.

In this paper, the users' houses are considered as thermal storages which can be pre-cooling or pre-warming in summer or winter before the coming of high electricity price [40]. The power consumption model of air-conditioning is given by equation (14). An inductive method is adopted to formulate the thermal model of a building. In order to simplify the heat dynamic model, we consider that the building exchanging heat only with external environment and air-conditioning. Then, the energy balance for the indoor air is formulated as equation (15), where $C$ and $R$ represent the heat capacity and resistance. Temperature $T_e(\tau)$ and load $l_a(\tau)$ represent environment temperature and power of air-conditioning at time $\tau$.

$$0 \le l_{a,\tau} \le l_{a,m} \tag{14}$$

$$C \cdot \frac{dT(\tau)}{d\tau} - \frac{1}{R} \cdot (T_e(\tau) - T(\tau)) = -l_a(\tau) \tag{15}$$

The power consumption $l_a(t)$ is a piecewise function, while $T_e(t)$ is a slowly varying function within each time slot. Based on the above assumptions, we can transform equation (15) into an equivalent discrete time equation (16) through the integration from time $t_k$ to time $t_{k+1}$. The climate comfort is quantified as equation (17), which is computed as a summation of the deviation from desired temperature $T_\alpha$.

$$T(t_{k+1}) = T_e(t_{k+1}) - \frac{1}{C} \cdot l_a(t_k) - (T_e(t_k) - T(t_k)) \cdot e^{-\frac{1}{RC}} \tag{16}$$

$$f_{clim,comf} = \frac{1}{H} \cdot \sum_{k=1}^{H} (T(t_k) - T_\alpha)^2 \tag{17}$$

For washing machine, the power consumption function of idle and occupied modes can be represented as equation (18), where $t_s$ and $t_e$ represent the starting and ending time when the washing machine is occupied. We adopt the value of waiting time $f_{wait,comf}$ to represent waiting comfort, where $t_\alpha$ represents the predetermined time decided by users. Therefore, the comfort function $f_{comf}$ can be computed as equation (20).

$$l_{w,\tau} = \begin{cases} l_w & t_s \le \tau \le t_e \\ 0 & otherwise \end{cases} \tag{18}$$

$$f_{wait,comf} = |t_s - t_\alpha| \tag{19}$$

$$f_{comf} = f_{wait,comf} + f_{clim,comf} \tag{20}$$

For electrical storage, it is expected to be well charged and discharged state within a scheduling horizon and the corresponding real-time pricing strategy, which help users reduce the electricity cost. Consider the constraints of charging or discharging power $l_{b,\tau}$ and battery state $SOC_\tau$ (state of charge), we formulate the power consumption function as follows:

$$l_{b,md} \le l_{b,\tau} \le l_{b,mc} \tag{21}$$

$$SOC_l \le SOC_\tau \le SOC_u \tag{22}$$

$$l_{b,t_k} = (SOC_{t_{k+1}} - SOC_{t_k}) \cdot C_a \cdot (t_{k+1} - t_k)^{-1} \tag{23}$$

where $l_{b,md}$ and $l_{b,mc}$ are the maximum discharging and charging power. $SOC_l$ and $SOC_u$ represent the minimum and maximum $SOC$. For background appliance, such as refrigerator, it is slightly influenced by the indoor air temperature. The power consumption model can be formulated as equation (24), where $l_{r,c,\tau}$ is the constant power consumption. $\lambda T(\tau)$ represents the extra power due to indoor air temperature $T(\tau)$. In order to simulate the peak demand of energy consumption, $l_{r,c}(\tau)$ is set to an piecewise function as equation (25), where we have $l_{r,c,l} > l_{r,c,m} > l_{r,c,h}$.

$$l_{r,\tau} = l_{r,c}(\tau) + \lambda \cdot T(\tau) \tag{24}$$

$$l_{r,c}(\tau) = \begin{cases} l_{r,c,h} & if\ 17 \le \tau \le 19 \\ l_{r,c,m} & if\ 20 \le \tau \le 23 \\ l_{r,c,l} & otherwise \end{cases} \tag{25}$$

Considering the security of household grid, the total power consumption of the above-mentioned appliances are expected to be limited to $l_m$ shown as equation (26) at any time within the scheduling horizon.

$$-l_m \le l_{a,\tau} + l_{w,\tau} + l_{b,\tau} + l_{r,\tau} \le l_m \tag{26}$$

In the proposed framework, we encourage the penetration of renewable energy resources for the purpose of reducing greenhouse gases. The estimation of the PV power generator, denoted by $l_{pv}$, can be achieved by various maximum power point tracking (MPPT) techniques [44]. For simplicity of illustration purpose, power generated from PV generation is assumed to follow a uniform distribution as equation (27), where $r$ is randomly chosen from continuous interval [0, 1]. Tuples ($l_{pv,l,c}$, $l_{pv,u,c}$) and ($l_{pv,l,s}$, $l_{pv,u,s}$) represent the PV output power when the weather is cloudy or sunny. Time interval [$t_a$, $t_b$] is the operating time duration of PV generator. For these special users who own PV generator, we have the following assumptions indicating their behaviour of using electricity. For time interval [$t_k$, $t_{k+1}$], the local generated

energy is firstly consumed by user's own appliances and the surplus electricity (if any) will be sold back to the grid. The tolerance capacity of their household grid is high enough to support their ability of generating electricity.

$$l_{pv,\tau} = \begin{cases} \begin{cases} U[l_{pv,l,c}, l_{pv,u,c}] & if\ r < 0.5 \\ U[l_{pv,l,s}, l_{pv,u,s}] & otherwise \end{cases} & if\ t_a \le \tau \le t_b \\ 0 & otherwise \end{cases} \tag{27}$$

The decision vector of user side is represented by a hybrid encodings $\boldsymbol{X} = (\boldsymbol{X}_a, \boldsymbol{X}_w, \boldsymbol{X}_b)$ to achieve appliance commitment, which is depicted in Fig. 6. The sub-vector $\boldsymbol{X}_a$, $\boldsymbol{X}_w$, and $\boldsymbol{X}_b$ represent the load scheduling of the air conditioning, washing machine, and electrical storage. Each dimension of $\boldsymbol{X}_a$ and $\boldsymbol{X}_b$ is a continuous variable representing their operating power at each time slot, and each dimension of $\boldsymbol{X}_w$ is a discrete variable representing the starting time when the washing machine is occupied. Therefore, we naturally encode each chromosome of GA as $\boldsymbol{X}$. Due to the hybrid encodings, traditional operations, i.e., crossover and mutation operations, are expected to be transformed into a hybrid. For crossover operation, simulated binary crossover operation is adopted for $\boldsymbol{X}_a$ and $\boldsymbol{X}_b$ while discrete uniform crossover operation is adopted for $\boldsymbol{X}_w$. Likewise, polynomial mutation and discrete uniform mutation are adopted for $\boldsymbol{X}_a$, $\boldsymbol{X}_b$, and $\boldsymbol{X}_w$, respectively.

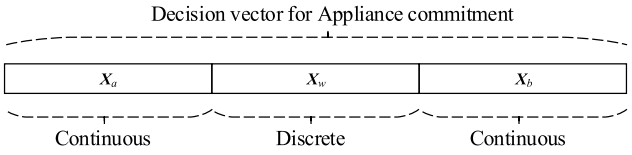


**FIGURE 6.** Hybrid representation of GA.

## III. EXPERIMENTAL RESULTS

In this section, three types of experiments are conducted to ascertain the performance of the proposed DCoEA. We first introduce the experimental setup, including the parameter settings and experimental platform in subsection *A*. In subsection *B*, we compare the DCoEA with other pricing strategies, such as the flat price and the random price. The comparisons are used to verify the effectiveness of DCoEA in terms of the improvement of profit and reduction of grid fluctuation. In subsection *C*, we investigate the performance of DCoEA when operator of top level considering different objectives, such as profit, fluctuation, and both of them. It should be noted that in order to ensure fairness when conducting this contrast experiment, SPSO of level II considers the same objectives (both grid fluctuation and net profit). In subsection *D*, we show the promising results of the appliance commitment conducted at user side. A three-level structure is adopted in the following experiment including one PWISO of level I, three RMGOs of level II, 30 users of level III (each RMGO regulates 10 users).

### A. EXPERIMENTAL SETUP

The DCoEA is tested on a computer cluster of 80 nodes (with the total of 320 processing cores), which are homogenous with the same Intel core i3-3240 CPU running at 3.40GHz, 4GB memory and Ubuntu 12.04 LTS 64-bit operating system. The parallel programing practice uses the Message Passing Interface (MPI).

All compared algorithms are conducted in 30 independent trials and the results are averaged over the trials. The nonparametric statistical tests [45], [46] conducted. The two-sided Wilcoxon rank sum test is adopted and conducted at significance level $\alpha = 0.05$. In the bottom of the experimental table, *w/t/l* represents that DCoEA achieves significantly superior, similar, and significantly inferior results than the compared algorithms.

Parameter settings are listed in Table 1. The parameters of SPSO and GA are set according to the suggestion of [42] and [43]. The maximum fitness evaluations ($FEs_{max}$) of level I, level II, and level II, are set to 2400, 600, and 200, respectively. Coefficient $\chi_1$ and $\chi_2$ are set to 0.13 and (195, 65) according to the practical value of ($f_{i,comf}$, $f_{i,cost}$) and ($f_{k,flu}$, $f_{k,prof}$), respectively. In the following experiments, we focus on investigating the solution quality of DCoEA. Therefore, $\varepsilon_m$ and $f_m$ are set to small and big enough in case of being terminated in advance before reaching the maximum number of FEs. Notation $\{k|k \in \mathbb{N}\}_r$ represents that integer $k$ is randomly chosen from a set of integers and $[a, b]_r$ is the continuous form. The *SOC* is limited to the range [10%, 95%], and the initial *SOC* of each user is randomly set at the range [10%, 20%]. The energy consumption of constant appliance is different at different time slots in order to simulate the peak electricity demand, i.e., 2.5 at time slots {17, 18, 19}, 1.5 at time slots {20, 21, . . . , 23}, and 0.5 at other time slots. Lower and upper bound of selling and purchasing price are set to different ranges, i.e., [0.13, 0.221] and [0.026, 0.13] for PWISO of level I, [0.13, 0.26] and [0.026, 0.13] for RMGOs of level II.

As can be noted from Table 1, the lower limit of selling price is higher than the upper limit of purchasing price. The special price setting protects PWISO and RMGOs from the scene where users can achieve huge profit by purchasing electricity at lower price and selling it back at higher price. Besides, the upper limit of selling price of RMGOs is a little higher than that of PWISO, which is expected to ensure the chance of RMGOs in making a profit.

### B. COMPARISON WITH FLAT AND RANDOM PRICING STRATEGY

In this subsection, we compare the DCoEA with two flat-price strategies and one random price strategy in order to ascertain the effectiveness of DCoEA in terms of the reduction of the grid fluctuation and enhance of the profit. In this experiment, the objectives of the SPSO of level I include both the fluctuation and the net profit, which is denoted by $FP_{bi}$. Table 2 shows the price settings of flat price strategy 1, flat

**TABLE 1. The parameter settings of the DCoEA. Notation "–*li*" represents the parameter settings of level *i*.**

| Parameter | Description | Value |
|---|---|---|
| $H$ | Length of Scheduling Horizon | 24 |
| $\chi_1$ | Coefficient to balance the order of magnitude | 0.13 |
| $\chi_2$-$l_{\mathrm{I}}$ | Coefficient to balance the order of magnitude (level I) | 195 |
| $\chi_2$-$l_{\mathrm{II}}$ | Coefficient to balance the order of magnitude (level II) | 65 |
| $\varepsilon_m$ | Maximum acceptable degree of fluctuation | 0 |
| $f_m$ | Minimum acceptable profit | 100000 |
| $(a, b, c)$ | Coefficient of quadratic cost function | $(4000^{-1}, 0.2, 0)$ |
| $l_{a,m}$ | Maximum rated power of air-conditioning | 5.0 |
| $(C, R)$ | Thermodynamic parameters | (2.0, 1.25) |
| $t_s$ | Starting time of washing machine | $\{0, 1, \ldots, 21\}_r$ |
| $t_e$-$t_s$ | Occupied time of washing machine | $\{1, 2\}_r$ |
| $[l_{w,min}, l_{w,max}]$ | Lower and upper bound of $l_w$ | [3.5, 5.5] |
| $C_a$ | Battery capacity | 10 |
| $[SOC_l, SOC_u]$ | Lower and upper bound of $SOC$ | [10%, 95%] |
| $l_{r,c,h/m/l}$ | constant power consumption | 2.5/1.5/0.5 |
| $[t_a, t_b]$ | Operating interval of PV generator | [10, 16] |
| $[l_{pv,l,c}, l_{pv,u,c}]$ | Lower and upper bound of $l_{pv}$ when cloudy | [3.2, 8] |
| $[l_{pv,l,s}, l_{pv,u,s}]$ | Lower and upper bound of $l_{pv}$ when sunny | [9.6, 16] |
| $\lambda$ | Degree of influence by indoor air temperature | 0.02 |
| $(l_{b,md}, l_{b,mc})$ | upper bound of $l_b$ | (-12, 8.8) |
| $FEs_{max}$-$l_{\mathrm{I}}$ | Upper bound of FES for SPSO (level I) | 2400 |
| $FEs_{max}$-$l_{\mathrm{II}}$ | Upper limit of FES for SPSO (level II) | 600 |
| $FEs_{max}$-$l_u$ | Upper limit of FES for GA (user level) | 200 |
| $N_s$-$l_{\mathrm{I}}$ | Swarm size of SPSO (level I) | 6 |
| $N_s$-$l_{\mathrm{II}}$ | Swarm size of SPSO (level II) | 6 |
| $N_p$-$l_u$ | Population size of GA (user level) | 20 |
| $[L_{p,s}, U_{p,s}]$-$l_I$ | Lower and upper bound of selling price (level I) | [0.13, 0.221] |
| $[L_{p,s}, U_{p,s}]$-$l_{\mathrm{II}}$ | Lower and upper limit of selling price (level II) | [0.026, 0.13] |
| $[L_{p,p}, U_{p,p}]$-$l_{\mathrm{II}}$ | Lower and upper limit of purchasing price (level I) | [0.13, 0.26] |
| $[L_{p,p}, U_{p,p}]$-$l_{\mathrm{II}}$ | Lower and upper limit of purchasing price (level II) | [0.026, 0.13] |
| $l_m$ | Upper limit of power consumption for household grid | $[8.8, 13.2]_r$ |
| *SPSO-p* | Probability to determine whether to update topology | $(1- FEs_{max}\text{-}l_k^{-1})^3$ |
| *SPSO-c* | Speed up coefficient of SPSO | 0.5+ln2 |
| *SPSO-w* | Weight coefficient of SPSO | $(2\times\ln 2)^{-1}$ |
| $P_c$ | Crossover probability | 0.9 |
| $P_m$ | Mutation probability | $N_p$-$l_u^{-1}$ |
| $(Nc, N_m)$ | Coefficients of probability density functions | (20, 20) |

price strategy 2, and the random price strategy, which are denoted by $FP_{01}$, $FP_{02}$, and $FP_r$, respectively. Price $FP_r$ represents the initial trial price strategy without optimization. For the PWISO of level I, the selling and purchasing prices

**TABLE 2. Setting of flat and random price strategy.**

| Pricing strategy | PWISO of level I | RMGO of level II |
|---|---|---|
| $FP_{01}$ | (0.195, 0.078) | (0.208, 0. 078) |
| $FP_{02}$ | (0.182, 0. 078) | (0.208, 0. 078) |
| $FP_r$ | ([0.13, 0.221], [0.026, 0.13]) | ([0.13, 0.26], [0.026, 0.13]) |

are set to (0.195, 0.078), (0.182, 0.078) and ([0.13, 0.221], [0.026, 0.13]) for price strategy $FP_{01}$, $FP_{02}$ and $FP_r$ at each time slot. For the RMGO of level II, the selling and the purchasing prices are set to (0.182, 0.078), (0.208, 0.078) and ([0.13, 0.26], [0.026, 0.13]) for price strategy $FP_{01}$, $FP_{02}$, and $FP_r$ at each time slot.

The experimental results are shown in Table 3. Three types of cases are used in this experiment. Case "CA" represents that the objective is optimizing both of the grid fluctuation and netprofit as equation (6). Cases "CB" and "CC" represent that the objectives are minimizing the grid fluction and maximizing the net profit. As can be noted from Table 3, DcoEA significantly outperforms the other pricing strategies on all of the test cases.

The experimental results are shown in Fig. 7, where the $x$-axis represents the grid fluctuation of level I (computed as $\chi_2$-$l_{\mathrm{I}} \cdot f_{k,flu}$) and the $y$-axis represents the net profit ($f_{k,prof}$) of level I. The increasing directions of the x-axis and the y-axis represent the lower grid fluctuation and the higher net profit, respectively. As can be node from Fig. 7, the results of $FP_{bi}$ are mostly distributed in area A which is an arc area at the increasing direction of function $f(x) = \gamma x$ ($\gamma > 0$), representing the lower grid fluctuation and the higher net profit. The results of $FP_{01}$, $FP_{02}$, and $FP_r$ are mostly distributed in areas B, C, and D, respectively. The center of each area is highlight in red solid symbol. Areas B, C, and D are distributed in the bottom left of area A, which reveals the price strategy $FP_{bi}$ outperforms $FP_{01}$, $FP_{02}$, and $FP_r$ in terms of the reduction of grid fluctuation and the enhancement of net profit.

Fig. 8 shows the results of the peak shifting of level I (a) and level II (b) at each time slot when applying different price strategies, where $FP_{flu}$ represents the smart pricing generator of level I considering only grid fluctuation. In Fig. 8, the peak to average ratio when applying $FP_{flu}$, $FP_{01}$, $FP_{02}$, and $FP_R$ are 1.467, 1.606, 1.604, and 1.661. Therefore, $FP_{flu}$ outperforms $FP_{01}$, $FP_{02}$, and $FP_R$ in terms of reducing grid fluctuation. In Fig. 8, the peak to average ratio of $FP_{flu}$, $FP_{01}$, $FP_{02}$, and $FP_R$ are 1.580, 1.693, 1.606, and 1.785, which indicates that the smart pricing generator of level II effectively achieves peak shifting and therefore smooth the grid fluctuation from user level. Fig. 8 indicates that the cooperation between smart pricing generators of level I and level II smooth the grid fluctuation by shifting the peak load, whilst the flat price strategies are unable to achieve peak shaving and load leaving. Therefore, in the proposed framework, PWISO is able to achieve lower grid fluctuation. Furthermore, the total

**TABLE 3. Experimental results of different pricing strategies.**

| Case ID | | $FP_{01}$ | $FP_{02}$ | $FP_r$ | DCoEA |
|---|---|---|---|---|---|
| CA1 | Mean | 2.22e+02 | 2.65e+02 | 2.33e+02 | **-5.21e+02** |
| | Std | 4.50e+04 | 2.92e+04 | 1.98e+04 | 1.60e+03 |
| | $p$ | 3.02e-11 | 3.02e-11 | 3.02e-11 | - |
| CA2 | Mean | 1.61e+02 | 3.49e+02 | 2.23e+02 | **-6.01e+02** |
| | Std | 3.72e+04 | 4.17e+04 | 1.54e+04 | 1.62e+03 |
| | $p$ | 3.02e-11 | 3.02e-11 | 3.02e-11 | - |
| CA3 | Mean | 2.76e+02 | 3.23e+02 | 4.88e+02 | **-6.18e+02** |
| | Std | 3.55e+04 | 3.87e+04 | 1.67e+05 | 1.44e+03 |
| | $p$ | 3.02e-11 | 3.02e-11 | 3.02e-11 | - |
| CA4 | Mean | 3.81e+02 | 6.44e+02 | 5.82e+02 | **-6.59e+02** |
| | Std | 2.53e+04 | 7.20e+04 | 8.91e+05 | 1.51e+03 |
| | $p$ | 3.02e-11 | 3.02e-11 | 3.02e-11 | - |
| CA5 | Mean | 6.38e+02 | 6.32e+02 | 3.70e+02 | **-6.81e+02** |
| | Std | 1.10e+05 | 840e+04 | 4.93e+04 | 1.76e+03 |
| | $p$ | 3.02e-11 | 3.02e-11 | 3.02e-11 | - |
| CB1 | Mean | 1.79e+00 | 1.66e+00 | 1.64e+00 | **1.39e+00** |
| | Std | 1.68e-02 | 9.16e-03 | 1.93e-02 | 2.67e-04 |
| | $p$ | 3.34e-11 | 4.62e-10 | 1.69e-09 | - |
| CB2 | Mean | 2.03e+00 | 1.95e+00 | 1.87e+00 | **1.62e+00** |
| | Std | 1.01e-01 | 8.72e-02 | 8.08e-02 | 5.41e-02 |
| | $p$ | 4.50e-11 | 6.07e-11 | 8.10e-10 | - |
| CB3 | Mean | 2.10e+00 | 2.00e+00 | 2.12e+00 | **1.67e+00** |
| | Std | 1.37e-01 | 1.27e-01 | 1.74e-01 | 8.27e-02 |
| | $p$ | 3.02e-11 | 3.02e-11 | 3.69e-11 | |
| CB4 | Mean | 2.22e+00 | 2.17e+00 | 2.12e+00 | **1.69e+00** |
| | Std | 1.51e-01 | 1.54e-01 | 1.76e-01 | 9.15e-02 |
| | $p$ | 3.02e-11 | 3.02e-11 | 2.37e-10 | - |
| CB5 | Mean | 2.35e+00 | 2.20e+00 | 2.03e+00 | **1.67e+00** |
| | Std | 1.99e-01 | 1.88e-01 | 1.76e-01 | 9.51e-02 |
| | $p$ | 3.34e-11 | 3.02e-11 | 9.76e-10 | - |
| CC1 | Mean | 2.46e+03 | 2.22e+03 | 2.46e+03 | **2.70e+03** |
| | Std | 5.27e+02 | 6.02e+03 | 3.69e+03 | 2.21e+03 |
| | $p$ | 1.56e-08 | 3.68e-11 | 6.52e-09 | - |
| CC2 | Mean | 2.89e+03 | 2.58e+03 | 2.89e+03 | **3.25e+03** |
| | Std | 1.70e+05 | 1.41e+05 | 1.84e+05 | 2.13e+03 |
| | $p$ | 1.07e-07 | 3.34e-11 | 3.09e-06 | - |
| CC3 | Mean | 2.87e+03 | 2.69e+03 | 2.95e+03 | **3.32e+03** |
| | Std | 2.65e+05 | 2.13e+05 | 2.66e+05 | 3.54e+03 |
| | $p$ | 5.19e-07 | 2.61e-10 | 5.46e-06 | - |
| CC4 | Mean | 2.95e+03 | 2.61e+03 | 2.94e+03 | **3.32e+03** |
| | Std | 2.74e+05 | 2.38e+03 | 2.92e+05 | 3.54e+03 |
| | $p$ | 3.81e-07 | 3.02e-11 | 3.96e-08 | - |
| CC5 | Mean | 2.88e+03 | 2.68e+03 | 2.97e+03 | **3.32e+03** |
| | Std | 2.94e+05 | 2.31e+05 | 2.99e+05 | 3.67e+03 |
| | $p$ | 5.07e-10 | 3.02e-11 | 4.57e-09 | - |
| *w/t/l* | - | 15/0/0 | 15/0/0 | 15/0/0 | - |

energy consumptions of Fig. 8(a) when conducting $FP_{flu}$, $FP_{01}$, $FP_{02}$, and $FP_R$ are 23839, 24218, 24304, and 24205, respectively. There are not significant differences between the total energy consumptions of different price strategies. The application of price strategy $FP_{flu}$ does not bring about the enhancement of total energy consumption, i.e., the developed pricing strategy does not burden the electricity grid.

### C. COMPARISON WITH DCoEA OF DIFFERENT OBJECTIVE

In this subsection, we investigate the performance of DCoEA when PWISO considers different objectives. Notations $FP_{flu}$, $FP_{prof}$, and $FP_{bi}$ represent that the objectives of SPSO (level I) are reducing the grid fluctuation, enhancing net profit, and both of them.

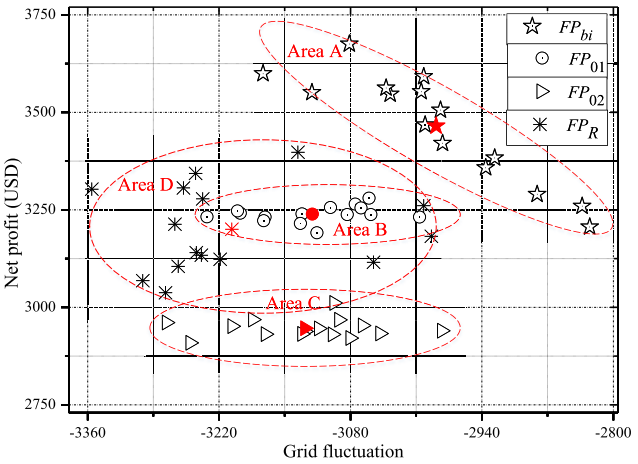


**FIGURE 7. Relationship between grid fluctuation and net profit when applying different price strategies. The solutions obtained by different pricing strategies are separately circled by the red dashed lines, and the solution distributions are denoted by area A, B, C, D. The centres of different areas are marked in red solid symbol.**

The experimental results are shown in Fig. 9. As can be noted from the scatter diagram, results of $FP_{flu}$ are mostly distributed in area $E$ along with a higher value in the increasing direction of $x$-axis, which represents a significant improvement in terms of the reduction of grid fluctuation. Results of $FP_{prof}$ are mostly distributed in area $F$ along with a higher value in the increasing direction of $y$-axis, which represents a significant enhancement in terms of net profit. The coordinate value $(-2989, 3465)$ of the center of area $A$ is intermediate between the value of area $E$ $(-2867, 3203)$ and $F$ $(-3146, 3602)$. Therefore, result of $FP_{bi}$ is a trade-off between the reduction of grid fluctuation and enhancement of net profit. It indicates that DCoEA allows system operators to consider different objectives, i.e., higher economic profit can be achieved at the cost of higher grid fluctuation, while lower grid fluctuation can be achieved by sacrificing economic profit.

As for load shifting, Fig. 10(a) gives an illustration of the results of level I. The peak to average ratio of $FP_{flu}$, $FP_{bi}$, and $FP_{prof}$ are 1.467, 1.529, and 1.605. Therefore, strategy $FP_{flu}$ achieves significantly higher efficiency than $FP_{bi}$ and $FP_{prof}$ in terms of reducing grid fluctuation. Fig. 10(b) shows the results of peak shifting for level II. The peak to average ratio of $FP_{flu}$, $FP_{bi}$, and $FP_{prof}$ are 1.580, 1.541, and 1.519, which indicates that level II achieves similar results when PWISO of level I considering different objectives. Furthermore, compared with results shown in Fig. 8(b), SPSO of level II achieves lower grid fluctuation than traditional price strategy.

### D. APPLIANCE COMMITMENT AT USER SIDE

In this subsection, we investigate the effectiveness of the smart scheduler of the user side. The classical GA is modified to conduct appliance commitment in order to help users

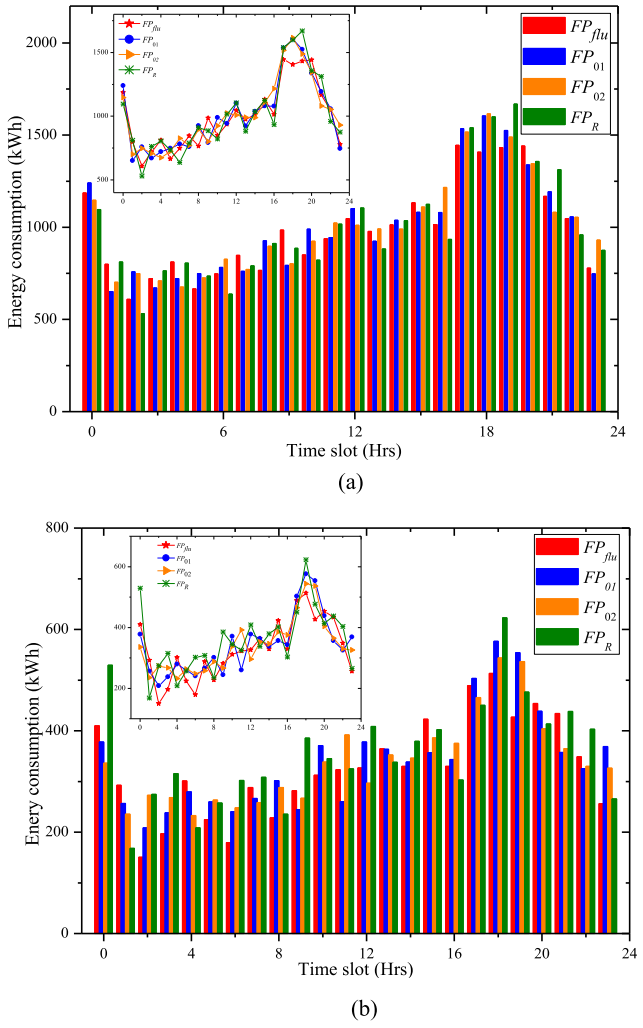


**FIGURE 8.** Results of the peak shifting of level I (a) and level II (b) when applying different price strategies.

achieve cost reduction while ensuring a high degree of comfort level. The experimental results indicate that the smart scheduler achieves cost reduction and enhances the comfort level for end users.

Since the SPSO of level II obtains approximate results under different price strategies of level I, we adopt $FP_{flu}$ in this experiment without the loss of fairness. With a given selling and purchasing price released from level II, Fig. 11 and Fig. 12 show the load shifting of electrical storage and air conditioning. In Fig. 11, *l-net* represents the total energy consumption without battery system. It can be noted that household battery tends to be charged at lower selling price (such as time slots [0, 1], [2, 3], [6, 7], [13, 14], and [16, 17]) and discharged at higher selling price (such as time slots [1, 2], [4, 5], [7, 8], [14, 15], and [19, 20]), which helps the users save electricity costs. Fig. 12 shows power schedule of air conditioning, ensuring that the inner air temperature is not higher than 30 centigrade, which is considered as an acceptable range.

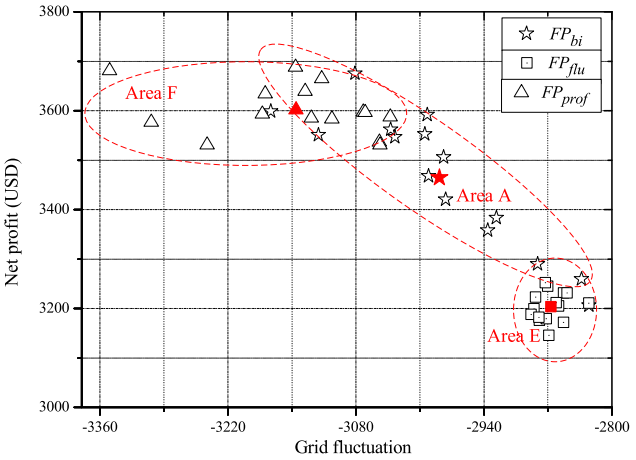


**FIGURE 9.** Relationship between grid fluctuation and net profit when applying different pricing strategies. The solutions obtained by different pricing strategies are separately circled by the red dashed lines, and the solution distributions are denoted by area A, B, C. The centres of different areas are marked in red solid symbol.

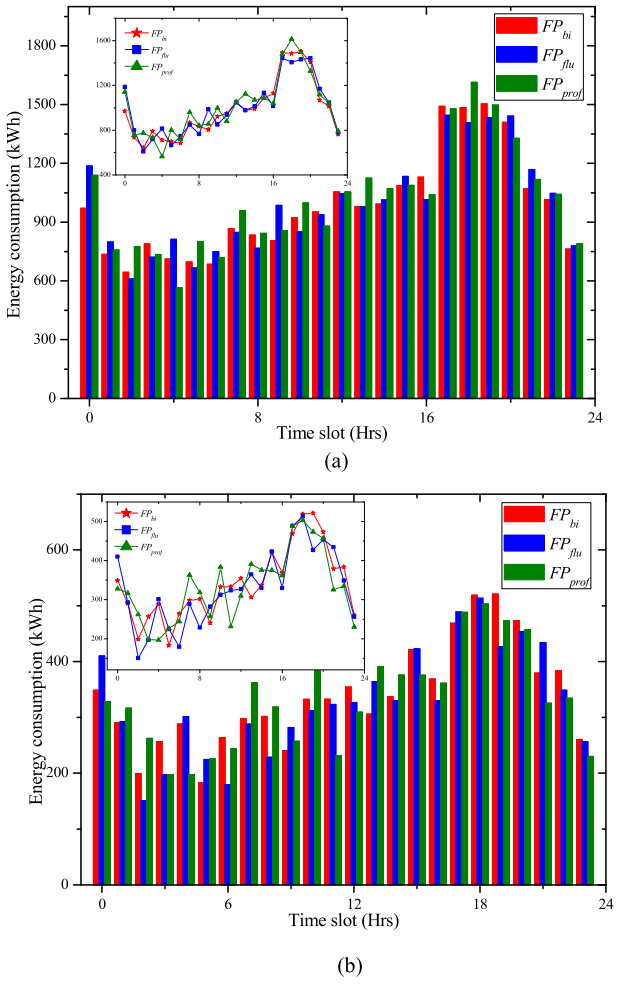


**FIGURE 10.** Results of peak shifting of level I(a) and level II(b) when applying different pricing strategies.

The scheduling of electrical storages, such as PHEVs, is crucial in reducing grid fluctuation. In the proposed framework, charging and discharging state of electrical storage is

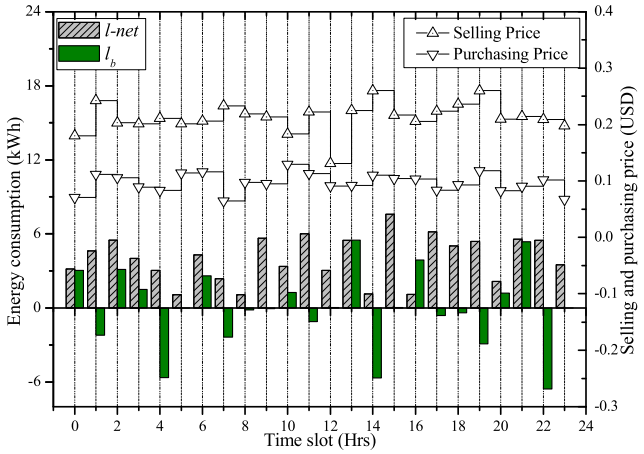


**FIGURE 11.** Battery load shifting according to selling and purchasing electricity price.

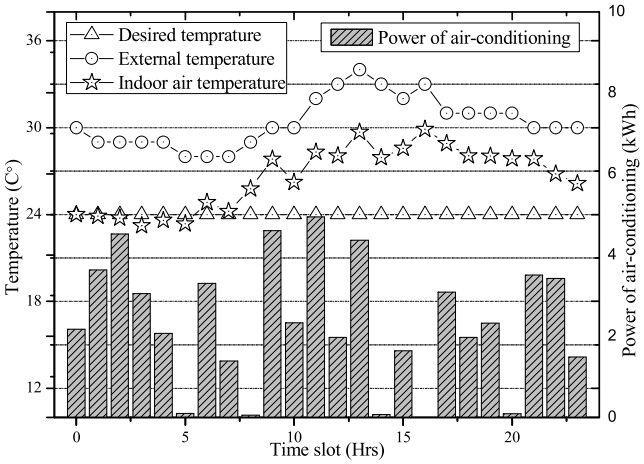


**FIGURE 12.** Indoor air temperature control via the scheduling of air-conditioning.

determined according to the released price information at user side. In order to ascertain the effectiveness of the pricing strategy developed by smart pricing generator, we investigate and show an overview of the charging and discharging response of electrical storages. In order to clearly show the charging and discharging response, we adopt single objective (the reduction of grid fluctuation) for smart pricing generator of level II and investigate the charging and discharging response of all users' electrical storages under a same RMGO. Fig. 13 shows the experimental results, where L-net is the net energy consumption without batteries, L-Tb is the total energy consumption of the batteries, and L-cb is the total energy consumption considering batteries. If all the electrical storages are viewed as a big storage, it tends to be charged when electricity price is low (such as time slots [0, 2], [7, 8], [11, 13], [16, 17], and [20, 23), and discharged when the electricity price is high (such as time slots [2, 3], [6, 7], [10, 11], [13, 14], and [17, 20]). The charging and discharging response of batteries reveals the regulative ability of pricing strategy developed by the smart pricing generator.

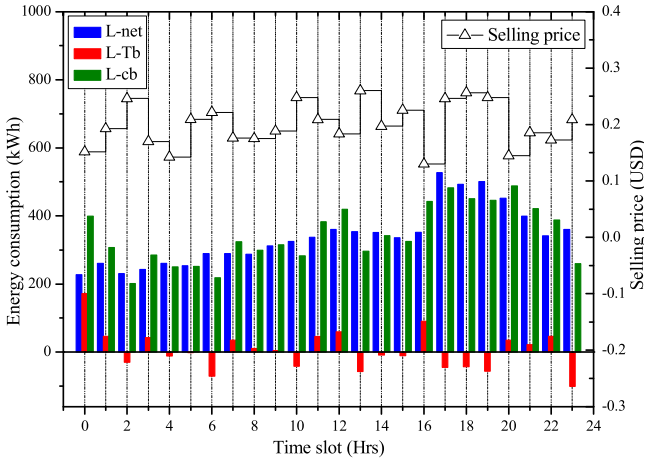


**FIGURE 13.** Overview of load shifting of all the storages at user level under a same RMGO.

## IV. CONCLUSION

In this paper, we propose a distributed co-evolutionary algorithm in order to cope with the complex landscape of problem space in smart grid. The management system is modeled as a hierarchical structure. Pricing information flows from the top level to the bottom level, whereas the energy consumption information flows from the bottom level to the top level. Therefore, upper level is able to guide the feedback of the energy consumption by appropriate pricing strategies. Communication process between adjacent levels is considered as an evolutionary gaming process, which is motivated from evolutionary game theory.

Three types of experiments have been conducted in order to verify the design and effectiveness of the proposed framework. For operator side, experimental results indicate the PSO-based smart pricing generator achieves higher economic profit and lower grid fluctuation than traditional pricing strategies. Besides, it allows trade-off between different objectives. For end users, GA is modified and applied to appliance commitment. Experimental results indicate the GA-based smart scheduler achieves cost reduction while ensuring high degree of comfort. The response of smart scheduler reveals the regulative ability of smart pricing generator.

Future work includes the development of an improved auxiliary operation to reduce the computational complexity, and the application of this framework to real-world problems.

## REFERENCES

[1] M. H. Albadi and E. F. El-Saadany, "A summary of demand response in electricity markets," *Electr. Power Syst. Res.*, vol. 78, no. 11, pp. 1989–1996, 2008.
[2] R. Deng, Z. Yang, M. Chow, and J. Chen, "A survey on demand response in smart grids: Mathematical models and approaches," *IEEE Trans. Ind. Informat.*, vol. 11, no. 3, pp. 570–582, Jun. 2015.
[3] J. S. Vardakas, N. Zorba, and C. V. Verikoukis, "A survey on demand response programs in smart grids: Pricing methods and optimization algorithms," *IEEE Commun. Surv. Tuts.*, vol. 17, no. 1, pp. 152–178, Mar. 2015.
[4] H. Allcott, *Real Time Pricing and Electricity Markets*. Cambridge, MA, USA: Harvard Univ., Jan. 2009.

[5] M. Doostizadeh and H. Ghasemi, "A day-ahead electricity pricing model based on smart metering and demand-side management," *Energy*, vol. 46, no. 1, pp. 221–230, Oct. 2012.

[6] S. Kim and G. B. Giannakis, "An online convex optimization approach to real-time energy pricing for demand response," *IEEE Trans. Smart Grid*, vol. 8, no. 6, pp. 2784–2793, Nov. 2017.

[7] S. Kwon, L. Ntaimo, and N. Gautam, "Optimal day-ahead power procurement with renewable energy and demand response," *IEEE Trans. Power Syst.*, vol. 32, no. 5, pp. 3924–3933, Sep. 2017.

[8] J. M. Guerrero, P. C. Loh, M. Chandorkar, and T.-L. Lee, "Advanced control architectures for intelligent microgrids—Part I: Decentralized and hierarchical control," *IEEE Trans. Ind. Electron.*, vol. 60, no. 4, pp. 1254–1262, Apr. 2013.

[9] W. Saad, Z. Han, H. V. Poor, and T. Basar, "Game-theoretic methods for the smart grid: An overview of microgrid systems, demand-side management, and smart grid communications," *IEEE Signal Process. Mag.*, vol. 29, no. 5, pp. 86–105, Sep. 2012.

[10] D. Pudjianto, C. Ramsay, and G. Strbac, "Virtual power plant and system integration of distributed energy resources," *IET Renew. Power Gener.*, vol. 1, no. 1, pp. 10–16, Mar. 2007.

[11] A. Mnatsakanyan and S. W. Kennedy, "A novel demand response model with an application for a virtual power plant," *IEEE Trans. Smart Grid*, vol. 6, no. 1, pp. 230–237, Jan. 2015.

[12] E. Mashhour and S. M. Moghaddas-Tafreshi, "Bidding strategy of virtual power plant for participating in energy and spinning reserve markets—Part I: Problem formulation," *IEEE Trans. Power Syst.*, vol. 26, no. 2, pp. 949–956, May 2011.

[13] W. Tushar *et al.*, "Three-party energy management with distributed energy resources in smart grid," *IEEE Trans. Ind. Electron.*, vol. 62, no. 4, pp. 2487–2498, Apr. 2015.

[14] M. M. Yu and S. H. Hong, "A real-time demand-response algorithm for smart grids: A Stackelberg game approach," *IEEE Trans. Smart Grid*, vol. 7, no. 2, pp. 879–888, Mar. 2016. doi: 10.1109/TSG.2015.2413813.

[15] N. H. Tran, D. H. Tran, S. Ren, Z. Han, E. Huh, and C. S. Hong, "How GEO-distributed data centers do demand response: A game-theoretic approach," *IEEE Trans. Smart Grid*, vol. 7, no. 2, pp. 937–947, Mar. 2016.

[16] S. Maharjan, Q. Zhu, Y. Zhang, S. Gjessing, and T. Basar, "Demand response management in the smart grid in a large population regime," *IEEE Trans. Smart Grid*, vol. 7, no. 1, pp. 189–199, Jan. 2016.

[17] C. Lee, L. Park, and S. Cho, "Light-weight stackelberg game theoretic demand response scheme for massive smart manufacturing systems," *IEEE Access*, vol. 6, pp. 23316–23324, 2018.

[18] S. Maharjan, Q. Zhu, Y. Zhang, S. Gjessing, and T. Basar, "Dependable demand response management in the smart grid: A Stackelberg game approach," *IEEE Trans. Smart Grid*, vol. 4, no. 1, pp. 120–132, Mar. 2013.

[19] A.-H. Mohsenian-Rad, V. W. S. Wong, J. Jatskevich, R. Schober, and A. Leon-Garcia, "Autonomous demand-side management based on game-theoretic energy consumption scheduling for the future smart grid," *IEEE Trans. Smart Grid*, vol. 1, no. 3, pp. 320–331, Dec. 2010.

[20] X. Chen, T. Wei, and S. Hu, "Uncertainty-aware household appliance scheduling considering dynamic electricity pricing in smart home," *IEEE Trans. Smart Grid*, vol. 4, no. 2, pp. 932–941, Jun. 2013.

[21] R. Fernandez-Blanco, J. M. Arroyo, N. Alguacil, and X. Guan, "Incorporating price-responsive demand in energy scheduling based on consumer payment minimization," *IEEE Trans. Smart Grid*, vol. 7, no. 2, pp. 817–826, Mar. 2015.

[22] Y. Z. Wang, X. Lin, and M. Pedram, "A stackelberg game-based optimization framework of the smart grid with distributed PV power and data centers," *IEEE Trans. Energy Convers.*, vol. 29, no. 4, pp. 978–987, Dec. 2014.

[23] S. Wang, S. Bi, and Y. A. Zhang, "Demand response management for profit maximizing energy Loads in real-time electricity market," *IEEE Trans. Power Syst.*, vol. 33, no. 6, pp. 6387–6396, Nov. 2018.

[24] L. P. Qian, Y. J. A. Zhang, J. W. Huang, and Y. Wu, "Demand response management via real-time electricity price control in smart grids," *IEEE J. Sel. Areas Commun.*, vol. 31, no. 7, pp. 1268–1280, Jul. 2013.

[25] J. Liu and J. Li, "A bi-level energy-saving dispatch in smart grid considering interaction between generation and load," *IEEE Trans. Smart Grid*, vol. 6, no. 3, pp. 1443–1452, May 2015.

[26] P. Faria, J. Soares, Z. Vale, H. Morais, and T. Sousa, "Modified particle swarm optimization applied to integrated demand response and DG resources scheduling," *IEEE Trans. Smart Grid*, vol. 4, no. 1, pp. 606–616, Mar. 2013.

[27] P. H. Nguyen, W. L. Kling, and P. F. Ribeiro, "A game theory strategy to integrate distributed agent-based functions in smart grids," *IEEE Trans. Smart Grid*, vol. 4, no. 1, pp. 568–576, Mar. 2013.

[28] Z. Y. Xu, W. S. Xu, W. H. Shao, and Z. Y. Zeng, "Real-time pricing control on generation-side: optimal demand-tracking model and information fusion estimation solver," *IEEE Trans. Power Syst.*, vol. 29, no. 4, pp. 1522–1535, Jul. 2014.

[29] S. Mhanna, A. C. Chapman, and G. Verbič, "A fast distributed algorithm for large-Scale demand response aggregation," *IEEE Trans. Smart Grid*, vol. 7, no. 4, pp. 2094–2107, Jul. 2016.

[30] S. Bahrami, M. H. Amini, M. Shafie-Khah, and J. P. S. Cataláo, "A decentralized electricity market scheme enabling demand response deployment," *IEEE Trans. Power Syst.*, vol. 33, no. 4, pp. 4218–4227, Jul. 2018.

[31] A. Kovács, "On the computational complexity of tariff optimization for demand response management," *IEEE Trans. Power Syst.*, vol. 33, no. 3, pp. 3204–3206, May 2018.

[32] B. Wang, X. Yang, T. Short, and S. Yang, "Chance constrained unit commitment considering comprehensive modelling of demand response resources," *IET Renew. Power Gener.*, vol. 11, no. 4, pp. 490–500, Mar. 2017.

[33] F. Rassaei, W. Soh, and K. Chua, "Distributed scalable autonomous market-based demand response via residential plug-in electric vehicles in smart grids," *IEEE Trans. Smart Grid*, vol. 9, no. 4, pp. 3281–3290, Jul. 2018.

[34] M. Diekerhof, F. Peterssen, and A. Monti, "Hierarchical distributed robust optimization for demand response services," *IEEE Trans. Smart Grid*, vol. 9, no. 6, pp. 6018–6029, Nov. 2018.

[35] S. Mhanna, A. C. Chapman, and G. Verbič, "A distributed algorithm for demand response with mixed-integer variables," *IEEE Trans. Smart Grid*, vol. 7, no. 3, pp. 1754–1755, May 2016.

[36] J. M. Smith, *Evolution and the Theory of Games*. Cambridge, U.K.: Cambridge Univ. Press, 1982.

[37] G. Q. Zeng, X.-Q. Xie, M.-R. Chen, and J. Weng, "Adaptive population extremal optimization-based PID neural network for multivariable nonlinear control systems," *Swarm Evol. Comput.*, vol. 44, pp. 320–334, Feb. 2019.

[38] G.-Q. Zeng, J. Chen, Y.-X. Dai, L.-M. Li, C.-W. Zheng, and M.-R. Chen, "Design of fractional order PID controller for automatic regulator voltage system based on multi-objective extremal optimization," *Neurocomputing*, vol. 160, pp. 173–184, Jul. 2015.

[39] P. Samadi, H. Mohsenian-Rad, R. Schober, and V. W. S. Wong, "Advanced demand side management for the future smart grid using mechanism design," *IEEE Trans. Smart Grid*, vol. 3, no. 3, pp. 1170–1180, Sep. 2012.

[40] M. Song, C. Gao, H. Yan, and J. Yang, "Thermal battery modeling of inverter air conditioning for demand response," *IEEE Trans. Smart Grid*, vol. 9, no. 6, pp. 5522–5534, Nov. 2018.

[41] I. Narayanan, D. Wang, A. Sivasubramaniam, and H. K. Fathy, "A stochastic optimal control approach for exploring tradeoffs between cost savings and battery aging in datacenter demand response," *IEEE Trans. Control Syst. Technol.*, vol. 26, no. 1, pp. 360–367, Jan. 2018.

[42] M. Clerc. (2012). *Standard Particle Swarm Optimization*. [Online]. Available: http://clerc.maurice.free.fr/pso/SPSO_descriptions.pdf

[43] K. Deb and R. B. Agrawal, "Simulated binary crossover for continuous search space," *Complex Syst.*, vol. 9, no. 2, pp. 115–148, 1995.

[44] B. Subudhi and R. Pradhan, "A comparative study on maximum power point tracking techniques for photovoltaic power systems," *IEEE Trans. Sustain. Energy*, vol. 4, no. 1, pp. 89–98, Jan. 2013.

[45] J. Derrac, S. García, D. Molina, and F. Herrera, "A practical tutorial on the use of nonparametric statistical tests as a methodology for comparing evolutionary and swarm intelligence algorithms," *Swarm Evol. Comput.*, vol. 1, no. 1, pp. 3–18, Mar. 2011.

[46] L. M. Li, K. D. Lu, G. Q. Zeng, L. Wu, and M. R. Chen, "A novel real-coded population-based extremal optimization algorithm with polynomial mutation: A non-parametric statistical study on continuous optimization problems," *Neurocomputing*, vol. 174, pp. 577–587, Jan. 2016.

**XINYUAN ZHANG** (S'14) received the B.S. degree from Sun Yat-sen University, China, in 2014, where he is currently pursuing the Ph.D. degree. His current research interests include evolutionary computation algorithms, swarm intelligence algorithms, large-scale optimization, their applications in real-world problems, and smart grid.

**YUE-JIAO GONG** (S'10–M'15) received the B.S. and Ph.D. degrees in computer science from Sun Yat-sen University, China, in 2010 and 2014, respectively. From 2015 to 2016, she was a Postdoctoral Research Fellow with the Department of Computer and Information Science, University of Macau, Macau. She is currently a Professor with the School of Computer Science and Engineering, South China University of Technology, China. Her research interests include evolutionary computation, swarm intelligence, and their applications to intelligent transportation scheduling. She has published over 70 papers, including more than 20 IEEE Transactions papers, in her research area.

**YUREN ZHOU** received the B.Sc. degree in mathematics from Peking University, Beijing, China, in 1988, and the M.Sc. degree in mathematics and the Ph.D. degree in computer science from Wuhan University, Wuhan, China, in 1991 and 2003, respectively. He is currently a Professor with the School of Data and Computer Science, Sun Yat-sen University, Guangzhou, China.

His current research interests include design and analysis of algorithms, and evolutionary computation.

**YING LIN** (M'13) received the Ph.D. degree in computer science from Sun Yat-sen University, China, in 2012, where she is currently an Assistant Professor with the Department of Psychology. Her main research interest includes computational intelligence and its applications in psychometrics and neuroimaging.